RP Current Trends In Applied Sciences
Vol. 3, No. 2 (April – June 2024) pp. 20–28
e-ISSN: 2583-7486

Cite this article: N. Singh, Quantum corrections on parametric interactions in ion-implanted semiconductor plasmas, *RP Cur. Tr. Appl. Sci.* **3** (2024) 20–28.

Original Research Article

Quantum corrections on parametric interactions in ion-implanted semiconductor plasmas

Navneet Singh*
Department of Physics, Rajiv Gandhi Government College for Women, Bhiwani 127021, Haryana, India
*Corresponding author, E-mail: ndhanda16@gmail.com

ARTICLE HISTORY
Received: 4 Jan. 2024
Revised: 28 March 2024
Accepted: 3 April 2024
Published online: 10 April 2024

KEYWORDS
Quantum effects; Parametric interactions; Ion-implantation; Semiconductor plasma; Hydrodynamic model; Coupled mode theory; Bohm potential; Rotating wave approximation.

ABSTRACT
Using the quantum hydrodynamic (QHD) model of semiconductor plasmas and the coupled mode theory of interacting waves, an analytical investigation is made to study the parametric interactions in semiconductor quantum plasmas, whose main constituents are the drifting electrons and non-drifting negatively-charged colloidal particles. The phenomenon of parametric interaction is treated as a three-wave interaction process, involving second-order nonlinearity of the medium. It is found that the second-order optical susceptibility in ion-implanted semiconductor quantum plasma is modified due to the presence of non-drifting charged colloidal particles. The inclusion of QEs is being done in the analysis via quantum correction term in classical hydrodynamic model of homogeneous semiconductor plasma. The effect is associated with purely quantum origin using quantum Bohm potential and quantum statistics. The colloidal size and the quantum correction term modify the parametric amplification characteristics of ion implanted semiconductor plasma medium. Numerical estimates made for n-InSb-CO_2 laser system exhibit that the QEs on colloids is inversely proportional to their size. Moreover critical size of implanted colloids for the effective quantum correction is determined which is found to be equal to the lattice spacing of the crystal. The present study also suggests that a proper selection of colloid density will lead to anomalous dispersion, which in turns becomes helpful in the generation of squeezed states. It is hoped that the present study may add substantially to the present knowledge of wave interaction and may become useful in designing the semiconducting devices.

1. Introduction

Parametric interactions in semiconducting materials have been studied by a number of researchers [1-10]. These interactions provide useful information regarding the physical properties of the host medium. A variety of nonlinear effects have been observed in the interaction of high-power electromagnetic waves with semiconductor plasmas.

Ion implantation is one of the most widely used doping techniques in the preparation of doped semiconductors with controlled impurity profiles. However, the crystal lattice is damaged during the implantation process and post implantation annealing becomes necessary to achieve a good degree of lattice recovery and electrical activation of the dopants. The implanted ions in a host material can modify physical property, viz., the high magnetic coercivity and nonlinear optical properties [11-14]. Hence, its main application lies in the manufacturing of semiconductor components. At low energy, chemical binding effects associated with ion-ion and ion-target atom interactions may explain the depth profile of implanted ion [13]. This process is responsible for the implanted metal ions being neutralized during the slowing down (electronic and nuclear stopping) processes and somehow agglomerating to form colloids of implanted materials.

However, if the colloid particles could somehow be aligned in a long range periodic manner; the host material would show a variety of useful thermodynamic, electrical and optical properties that can be easily manipulated. The ion implantation is a well known technique for versatile nanofabrication tool. In recent years, a number of workers [15-18] have theoretically studied the long range order lattice formation of colloid particle of small sizes in piezoelectric semiconductors.

The presence of external drift field well below the breakdown of the semiconductor may drive a beam of electrons with a drift speed comparable to the ion-acoustic phonon speed in the crystal. These external fields induce uniform electron current that may charge the as grown colloid particles by sticking collisions. By this process colloidal plasma will be formed with electrons, negatively charged colloid particles and vibrating positive lattice ion centers, similar to the dusty plasma. This medium will turn as ion-implanted semiconductor plasma (IISP) medium. In recent past, the role of charged colloids in searching the novel modes of propagation and/or in modification of wave characteristics of existing modes in semiconductor plasma has been extensively explored [19-21]. Workers have established the existence of a number of novel modes as well as creative modifications in the characteristics of existing modes [19-21] of propagation. The current reports in the field also indicate that the presence of charged colloids have a strong influence on wave characteristics of existing modes even at frequencies where colloidal grains do not participate in the linear motion of waves. In such cases, the colloids provide an immobile charge neutralizing background in the medium.

To the best of authors' knowledge, the quantum effects (QEs) have been ignored in all the previous works reported for IISPs. However, for relatively large density of electrons in doped piezoelectric semiconductor, QEs may become very significant in IISPs. In the recent past, Zeba et al. [22] have reported the colloid crystal formation in semiconductor quantum plasma. They have shown that the dielectric response function of the semiconductor is contributed by QEs of electrons through Bohm potential and lattice electron-phonon coupling effects. QEs on modulation amplification and the dispersion, threshold and gain characteristics of Brillouin scattered Stokes mode (BSSM) have been studied in IISPs [23, 24]. But there is no report on the study of QEs on parametric interactions in IISPs till date.

Hence, study of the basic second order nonlinear wave interaction i.e. the parametric interaction in IISPs using QHD model of plasmas [25] appears to be quite promising. Using QHD model parametric amplification characteristics in piezoelectric semiconductor has been recently reported [1-10] studies the QEs on parametric amplification of acoustic phonons in semiconductor magneto-plasmas. Role of implanted charged colloids in parametric processes was reported by Ghosh et al. [5] in piezoelectric semiconductor plasmas. However, in this study, uniform sized colloids were considered. This size may be assumed to be smaller than the perturbation wavelength, inter-grain distance as well as electron Debye radius to simplify the problem without scarifying any essential information in general.

In fact, colloidal plasma consists of many different colloid grains with multiple sizes [26-29] in both the space plasma and the laboratory experiments. Most of the available literature deals with uniform size dust distribution but in nature we encounter with grains of multiple sizes. Such disparity demands the study of colloidal size distribution effect on parametric interactions in IISPs, which will form the basis of an adequate examination. It would also be worthwhile to examine the modifications in the dispersion characteristics of IISPs with respect to earlier works [1-10] using QHD model. In addition to QEs, dust size effect has also been incorporated to study parametric dispersion characteristics of IISPs which make this work a novel study with applications in optical signal processing and microelectronics industry.

2. Theoretical formulations

In this section, we focused on the second-order optical susceptibility arising due to parametric interaction of a high frequency pump beam with internally generated acoustic mode in an IISP with QEs. The medium is subjected to a spatially uniform high frequency pump electric field $\vec{E}_0 \exp(-i\omega_0 t)$ (i.e. pump vector $|\vec{k}_0| = 0$). We could neglect the non-uniformity of the high frequency pump field under dipole approximation when the excited acoustic waves have wavelength small compared to the scale-length of the electromagnetic field variation [30]. We have considered colloids-rich piezoelectric semiconductor quantum plasma as a medium under study with a view to control the parameters easily.

The carrier dynamics is described by a set of hydrodynamic equations (typically, continuity and momentum transfer) that include QEs via a Bohm-like potential. Quantum statistics and the new force associated with quantum Bohm potential introduce the pressure effects of pure quantum origin. The quantum hydrodynamic (QHD) model is a reduced model that allows straightforward investigation of the collective dynamics rather than to deal with complexities of Schrodinger-Poisson (2N equations) or Wigner Poisson (phase space dynamics) models.

The condition for charge neutrality in medium with negatively charged colloids is given by

$$n_{0i} = Z_{0d} n_{0d} + n_{0e} \tag{1}$$

where n_{0i}, n_{0e} and n_{0d} are the number densities of unperturbed ions, electrons and the colloid grain, respectively. Z_{0d} is the unperturbed number of charges residing on the colloid grain measured in units of electron charge.

Due to the fact that when plasma is cooled down to an extremely low temperature, the de-Broglie wavelength of the charge carriers can be comparable to the dimension of the system, the ultra-cold colloidal plasma behaves like a Fermi gas and one dimensional Fermi gas obeys the pressure law [31]. The quantum statistics is included in the model via the equation of state which has been slightly modified to include Fermionic character of the colloids as:

$$P_{Fj} = \frac{m_j V_{Fj}^2 n_{1j}^3}{3 n_{0j}^2} \tag{2a}$$

$l = e$ (electrons) and d (colloids with different grain size). P_{Fj} is the Fermi pressure, m_j is the effective mass, V_{Fj} is the Fermi speed; n_{0j} and n_{1j} stand for the equilibrium and perturbed plasma carrier density, respectively. The Fermi pressure is interpreted as a result of velocity dispersion around mean velocity of the plasma particles. It may be obtained by assuming the zero-temperature Fermi distribution of plasma particles. In terms of Fermi temperature T_F, Fermi speed may be expressed as [32]:

$$V_{Fj} = \frac{2k_B T_F}{m_j}. \tag{2b}$$

We consider an IISP system composed of electrons and negatively charged colloids. In this situation the one dimensional QHD model [33, 34] consists of the continuity and the momentum balance equations along with Poisson's equation which are as follows:

$$\frac{\partial^2 u(x,t)}{\partial t^2} - 2\Gamma_a \frac{\partial u(x,t)}{\partial t} + \frac{\beta}{\rho}\frac{\partial E_1}{\partial x} = \frac{C}{\rho}\frac{\partial^2 u(x,t)}{\partial x^2} \tag{3}$$

$$\frac{\partial v_{0j}}{\partial t} + \nu v_{0j} = -\frac{Z_j e}{m_j} E_0 \tag{4}$$

$$\frac{\partial v_{1l}}{\partial t} + \nu v_{1l} + \left(v_{0j} \cdot \frac{\partial}{\partial x} \right) v_{1j} = -\frac{Z_j e}{m_j} E_1 - \frac{1}{m_j n_0}\frac{\partial P_1}{\partial x} + \frac{\hbar^2}{4 m_j^2 n_{0j}} \frac{\partial^3 n_{1j}}{\partial x^3} \tag{5}$$

$$v_{0j}\frac{\partial n_{1j}}{\partial x}+n_{0j}\frac{\partial v_{1j}}{\partial x}=-\frac{\partial n_{1j}}{\partial t} \tag{6}$$

$$\frac{\partial E_1}{\partial x}+\frac{\beta}{\varepsilon}\frac{\partial^2 u}{\partial x^2}=-\frac{Z_j e n_{1j}}{\varepsilon}. \tag{7}$$

Equation (3) describes the motion of acoustic mode in an IISP. Here, C is the elastic constant, ρ is the mass density, Γ_a is the acoustic damping parameter, and β is the piezoelectric coefficient of IISP crystal. $u(x,t)$ is the lattice displacement and it may be expressed as: $u(x,t)=u\exp[i(k_a x-\omega_a t)]$. We assumed that the frequency of acoustic mode is much smaller than the frequency of pump wave, i.e. $\omega_a << \omega_0$. Equations (4) and (5) are the equations of motion expressing zeroth and first order oscillatory fluid velocities (v_{0j}, v_{1j}) of carriers with effective mass m_j and charge $Z_j e$. ν is the phenomenological carrier collision frequency and $Z_j=q_j/e$ is the charge state of electrons and colloids, which is the ratio of negative charges q_d resided over the colloidal grains to the charge e. The space charge field E_1 is determined by the Poisson equation (7) where ε is the dielectric constant of IISP medium. We have neglected the quantum diffraction effect; hence the charge density can be obtained from the potential through an algebraic equation [32] and Poisson equation should not be modified to include quantum contribution. In IISPs, the low frequency acoustic wave ω_a as well as the pump electromagnetic wave ω_0 produce density perturbations (n_1) at the respective frequency in the medium which can be obtained by using the standard approach [35]. Using equations (2) to (7) and considering the low-frequency perturbations (n_s) to be proportional to $\exp[i(k_a x-\omega_a t)]$, while n_0 and v_0 vary as $\exp(-i\omega_0 t)$, one gets:

$$\frac{\partial^2 n_{1l}}{\partial t^2}+(\omega_{pj}^2+k^2V_{Fj}^{'2})n_{1j}+\nu\frac{\partial n_{1e}}{\partial t}+\frac{Z_j e n_{0j}\beta}{m_j\varepsilon}\frac{\partial^2 u}{\partial x^2}=-\bar{E}_j\frac{\partial n_{1j}}{\partial x} \tag{8}$$

where $\bar{E}_j=-\left(\frac{Z_j e}{m_j}E_0\right)$, $V_{Fj}^{'}=V_{Fj}\sqrt{1+\gamma_{ej}}$, $\gamma_{ej}=\frac{\hbar^2k^2}{8m_j k_B T_{Fj}}$.

In the derivation of equation (8), we have neglected the Doppler shift under the assumption that $\omega_0 >> \nu > kv_0$; $\omega_{pj}=\left(\frac{(Z_j)^2 n_{0j}e^2}{m_j\varepsilon}\right)^{1/2}$ is the plasma frequency of carriers.

The perturbed carrier density n_{1j} produced in the medium has two components known as slow and fast ($n_{1j}=n_{sj}+n_{fj}$). The slow component $n_{sj}[\propto \exp i(k_s x-\omega_a t)]$ is associated with the acoustic phonon mode (ω_a, k_a) while the fast component $n_{fj}[\propto \exp i(k_s x-\omega_s t)]$ is associated with the high frequency scattered electromagnetic wave (ω_s, k_s), arising due to the parametric interaction. These waves will propagate at generated frequencies ω_a and $\omega_0\pm\omega_a$ respectively. We assume that the energy transfer between the pump and produced signal and idler waves satisfy phase matching conditions which are: $\omega_0=\omega_s+\omega_a$ and $\vec{k}_0=\vec{k}_s+\vec{k}_a$. We have restricted ourselves only to the Stokes component ($\omega_0-\omega_a$) of the scattered electromagnetic waves. By resolving equation (8) into two components (fast and slow) under the rotating wave approximation, we obtain the respective coupled equations as:

$$\frac{\partial^2 n_{fj}}{\partial t^2}+\nu\frac{\partial n_{fe}}{\partial t}+(\omega_{pj}^2+k^2V_{Fj}^{'2})n_{sj}=-\bar{E}_j\frac{\partial n_{sj}^*}{\partial x} \tag{9a}$$

$$\frac{\partial^2 n_{sj}}{\partial t^2}+\nu\frac{\partial n_{se}}{\partial t}+(\omega_{pj}^2+k^2V_{Fj}^{'2})n_{sj}+\frac{Z_j e n_{0j}\beta}{m_j\varepsilon}\frac{\partial^2 u}{\partial x^2}=-\bar{E}_j\frac{\partial n_{fj}^*}{\partial x} \tag{9b}$$

subscripts s and f stand for slow and fast components, respectively. Asterisk (*) represents complex conjugate of the quantity.

It is clear from equations (9a) and (9b) that the slow and fast components of the density perturbations are coupled to each other via the pump electric field.

2.1 Second-order optical susceptibility due to electrons

In order to avoid complexities separate formulations have been done for electrons and charged colloids in the IISPs. We obtain slow component n_s for electron as:

$$n_s^*=\frac{-in_0 Z_e e\beta^2k^3E^*}{m\rho\varepsilon(\omega_a^2-k^2v_a^2-2i\Gamma_a\omega_a)}[R]^{-1} \tag{10}$$

where

$$R=\left[(\omega_{pe}^2+k^2V_{Fe}^{'2})-\omega_a^2-i\nu\omega_a-\frac{k^2\left|\bar{E}_e\right|^2}{(\omega_{pe}^2+k^2V_{Fe}^{'2})-\omega_s^2+i\nu\omega_s}\right]$$

The resonant component of the induced current density due to density perturbations oscillating at the acoustic frequency is given by

$$J_1=-n_s^*Z_e e v_0. \tag{11}$$

Using equation (10) we have

$$J_1=\frac{iZ_e e\varepsilon Ak\omega_{pe}^2E_0E^*}{2m\Gamma_a\omega_a\omega_0}[R]^{-1}. \tag{12}$$

where $A=K^2k^2v_a^2$, $K^2=\frac{\beta^2}{\varepsilon C}$, $\omega_s=\omega_0-\omega_a$,

$v_0=\frac{\bar{E}_e}{(\nu-i\omega_0)}$, and $\omega_{pe}=\left(\frac{n_e e^2}{m_e\varepsilon}\right)^{1/2}$ electron plasma frequency.

In deriving equation (12), the components of oscillatory electron fluid velocity v_0 are obtained from equation (4). Henceforth, the induced polarization will be

$$P_e=\frac{-Z_e e\varepsilon Ak\omega_{pe}^2E_0E_1^*}{2m\Gamma_a\omega_a\omega_0\omega_s}[R]^{-1}=\varepsilon_0\chi_e^{(2)}E_0E_1^*. \tag{13}$$

From equation (13), one may obtain the lowest order nonlinear susceptibility including quantum mechanical effects as:

$$\chi_e^{(2)} = \frac{-Z_e e \varepsilon_1 A k \omega_{pe}^2 E_0 E_1^*}{2m\Gamma_a \omega_a \omega_0 \omega_s}[R]^{-1}. \tag{14}$$

Equation (14) gives the real $\mathrm{Re}(\chi_e^{(2)})$ and imaginary $\mathrm{Im}(\chi_e^{(2)})$ parts of susceptibility as:

$$\mathrm{Re}(\chi_e^{(2)}) = \frac{-Z_e e \varepsilon_1 A k \omega_{pe}^2}{2m\Gamma_a \omega_a \omega_0 \omega_s}[X] \tag{15a}$$

$$\mathrm{Im}(\chi_e^{(2)}) = \frac{Z_e e \varepsilon_1 A k \omega_{pe}^2}{2m\Gamma_a \omega_a \omega_0 \omega_s}[Y], \tag{15b}$$

in which

$$X = \frac{\delta_2^4\delta_1^2 - \delta_2^2 k^2 \left|\bar{E}\right|^2 + \delta_1^2 \omega_s \nu^2}{[\delta_1^2\delta_2^2 + \omega_s\omega_a\nu^2 - k^2\left|\bar{E}\right|^2]^2 + [\delta_2^2\omega_a\nu - \delta_1^2\omega_s\nu]^2}$$

$$Y = \frac{\delta_2^4\omega_a\nu + \omega_s^2\nu^3\omega_a - \omega_s\nu k^2\left|\bar{E}\right|^2}{[\delta_1^2\delta_2^2 + \omega_s\omega_a\nu^2 - k^2\left|\bar{E}\right|^2]^2 + [\delta_2^2\omega_a\nu - \delta_1^2\omega_s\nu]^2}.$$

It is seen that both dispersion as well as amplification characteristics of acoustic wave are effectively modified in quantum plasma through $\delta_1^2 = \omega_{pe}^2 + k^2 V_{Fe}^{'2} - \omega_a^2$ and $\delta_2^2 = \omega_{pe}^2 + k^2 V_{Fe}^{'2} - \omega_s^2$.

2.2 Second-order optical susceptibility due to implanted colloids

Due to high mobility of drifting electrons colloidal grains tend to acquire a net negative charge through sticking processes. On neglecting the higher harmonics, the Stokes mode of the scattered component at $(\omega_0 - \omega_a)$ can be obtained from equations (7) and (9) as:

$$n_s^* = \frac{-i n_{0d} Z_d e \beta^2 k^3 E_1^*}{m_d \rho\varepsilon(\omega_a^2 - k^2 v_a^2 - 2i\Gamma_a\omega_a)}[V]^{-1}, \tag{16}$$

in which

$$V = \left[\left(\frac{n_{0d}Z_d^2e^2}{m_d\varepsilon} + \frac{2k^2k_BT_{Fd}}{m_d} + \frac{k^4\hbar^2}{4m_d^2}\right) - \omega_a^2 - \frac{k^2\left|\bar{E}_d\right|^2}{\left(\frac{n_{0d}Z_d^2e^2}{m_d\varepsilon} + \frac{2k^2k_BT_{Fd}}{m_d} + \frac{k^4\hbar^2}{4m_d^2}\right) - \omega_s^2}\right].$$

The Stokes component of the induced current density due to charged colloids is given by

$$J_d = -n_s^* Z_d e v_{0d}. \tag{17}$$

Substituting equation (16) into equation (17), we get

$$J_d = \frac{i Z_d^3 e^3 n_{0d} A k E_0 E_1^*}{2m_d^2 \Gamma_a \omega_a \omega_0}[V]^{-1}. \tag{18}$$

where $A = K^2 k^2 v_a^2$, $\omega_s = \omega_0 - \omega_a$,

$$K^2 = \frac{\beta^2}{\varepsilon C}, \text{ and } v_{0d} = \frac{\bar{E}_d}{(-i\omega_0)}.$$

Using the relations between current density and polarization discussed in previous chapters, we get the induced polarization due to negatively charged colloids as:

$$P = \frac{-Z_d^3 e^3 n_{0d} A k E_0 E_1^*}{2m_d^2 \Gamma_a \omega_a \omega_0 \omega_s}[V]^{-1} = \varepsilon_0 \chi_d^{(2)} E_0 E_1^*. \tag{19}$$

From equation (19), one may obtain the second order nonlinear susceptibility due to colloids including quantum mechanical effects as:

$$\chi_d^{(2)} = \frac{-Z_d^3 e^3 n_{0d} A k}{2\varepsilon_0 m_d^2 \Gamma_a \omega_a \omega_0 \omega_s}[V]^{-1}. \tag{20}$$

Equation (20) also exhibits the real $\mathrm{Re}[\chi_d^{(2)}]$ and imaginary $\mathrm{Im}[\chi_d^{(2)}]$ parts of total optical nonlinear susceptibility due to implanted colloids as:

$$\mathrm{Re}[\chi_d^{(2)}] = \frac{-Z_d^3 e^3 n_{0d} A k}{2\varepsilon_0 m_d^2 \Gamma_a \omega_a \omega_0 \omega_s}[V]^{-1} \tag{21}$$

$$\mathrm{Im}[\chi_d^{(2)}] = 0. \tag{22}$$

Equation (21) represents the real part of susceptibility due to implanted charged colloids, but the imaginary part is found to be equal is zero.

2.3 Total susceptibility of medium

Addition of equations (14) and (20), gives the total optical nonlinear susceptibility of the medium including quantum mechanical effects as:

$$\chi_t^{(2)} = \frac{e\varepsilon_1 Ak}{2\Gamma_a\omega_a\omega_0\omega_s}\left[\frac{Z_e\omega_{pe}^2}{m_e}[R]^{-1} + \frac{Z_d\omega_{pd}^2}{m_d}[V]^{-1}\right], \qquad (23)$$

where $\omega_{pd} = \left(\frac{(Z_d)^2 n_d e^2}{m_d\varepsilon}\right)^{1/2}$ is dust plasma frequency.

Real $\mathrm{Re}[\chi_t^{(2)}]$ and imaginary $\mathrm{Im}[\chi_t^{(2)}]$ parts of the total nonlinear susceptibility of the medium is given as:

$$\mathrm{Re}[\chi_t^{(2)}] = \mathrm{Re}[\chi_e^{(2)}] + \mathrm{Re}[\chi_d^{(2)}]$$

$$= \frac{\varepsilon_1 Ak}{2\Gamma_a\omega_a\omega_0\omega_s}\left[\frac{Z_e e\omega_{pe}^2}{m_e}[X] + \frac{Z_d e\omega_{pd}^2}{m_d}[V]^{-1}\right]. \qquad (24a)$$

$$\mathrm{Im}[\chi_t^{(2)}] = \mathrm{Im}[\chi_e^{(2)}] + \mathrm{Im}[\chi_d^{(2)}]$$

$$= \frac{\varepsilon_1 Ak}{2\Gamma_a\omega_a\omega_0\omega_s}\left[\frac{Z_e e\omega_{pe}^2}{m_e}[Y] + 0\right]. \qquad (24b)$$

It may be inferred from equation (24) that the susceptibility due to implanted charged colloid $\chi_d^{(2)}$ makes an important impact on the real part of total crystal susceptibility, whereas the imaginary part of total crystal susceptibility (equation (24b)) is produced only due to majority charge carriers (electron) and implanted charged colloids does not induce any modification in it.

QE of the particles mainly depends upon their size and mass. Generally larger size and mass will give rise to smaller QEs. QE on electron dynamics are non-variant due to constant size and mass of the electrons but QE on colloids may become variant due to available variations in size and mass of colloids. The grains in colloidal plasma are found in a great variety of sizes, masses and charges. Hence the study of colloidal size distribution and its contribution to quantum correction of second order optical nonlinearities is inevitable.

2.4 Colloidal size management: Polynomial size distribution function

In equilibrium, the plasma is quasi-neutral and the quasi-neutrality condition in the basic state is given by

$$\frac{n_{0i}}{n_{0e}} = 1 + \frac{Z_{0d} n_{0d}}{n_{0e}}, \qquad (25)$$

where n_{0i}, n_{0e}, n_{0d} and Z_{0d} are the number densities of unperturbed ions, electrons, colloid grains and charges residing on the colloid respectively. In this proposed study we have considered that the charge on the colloid particles is only due to electron attachment.

The size and shape of colloid grains in plasma will be different, unless they are man-made. The dust particles in laboratory dusty plasmas may be mono-sized. The particles that are implanted can be made of either dielectric or conducting materials with a very narrow distribution of diameters. Such narrowly sized particles are termed mono-dispersed.

In the charge neutrality condition when $Z_{0d} n_{0d} / n_{0e}$ is much smaller than one, the colloid particles can be considered as isolated colloidal grains and charge residing on grain depends only on the colloid particle radius. The differential number density of charged colloid grain is suggested with a characteristic radial parameter r [36].

$$n_{0d} = n_{0d}(r)dr. \qquad (26)$$

Here $n_{0d}(r)dr$ denotes the number of charged colloid grain with radius r that is expected per unit volume.

The colloid grain effectively collect electrons and it measured in units of electron charge. When grain size r is much smaller than the Debye radius λ_D, we can express the mass and charge of a colloid particle with characteristics radial parameter by

$$m_d = k_m r^3 \qquad (27)$$

$$Z_d = k_z r, \qquad (28)$$

where $k_z = \frac{4\pi\varepsilon_0 V_0}{e}$, $k_m = \frac{4\pi\rho_d}{3}$, V_0 is the electric surface potential at equilibrium, ρ_d is the mass density of the colloid grains (assumed to be constant and equal for all grains) and ε_0 is the vacuum permittivity.

It is assumed that the colloids are of multiple sizes and are smaller than the wavelength understudy as well as electron Debye radius. Hence they can be treated as negatively charged point masses. The colloid size distribution can be an arbitrary function in laboratory or even in the space plasma. The distribution function depends on many physical factors and on the environment. It has been widely accepted that the size distribution can be described by a power law distribution (PLD) in space plasma [37] and a Gaussian distribution in laboratory plasma, [38]. But generally, the colloid size distribution function does not exactly satisfy either a power law distribution or a Gaussian distribution. In our work we consider a polynomial expressed distribution of colloid particles in quantum colloidal plasma medium consisting of different size colloids. The differential polynomial expressed distribution function is of the form

$$n(r)dr = [a_0 + a_1 r + a_2 r^2 + ...]dr, \qquad (29)$$

where r is the radius of colloids in a given range [r_{min}, r_{max}], a_0 a_1 a_2 a_3 are all constant.

It satisfies the following equation:

$$N_{tot} = \int_{r_{\min}}^{r_{\max}} n(r)dr, \qquad (30)$$

where N_{tot} is the total number density of colloid grains. Outside the limits $r < r_{\min}$ and $r > r_{\max}$, we use $n(r) = 0$. We assume that the colloid size distribution is given by equation (28) and (30) substituting into equation (20), we obtain

$$\int_{r_{\min}}^{r_{\max}} \chi_d^{(2)} dr = \int_{r_{\min}}^{r_{\max}} \frac{-Ae^3 k}{2\varepsilon_0 \Gamma_a \omega_a \omega_0 \omega_s} \frac{k_z^3}{k_m^2} \frac{n(r)}{r^3} [Z]^{-1} dr \,, \tag{31}$$

in which

$$Z = \left[\left(\frac{e^2}{\varepsilon} \frac{k_z^2}{k_m} \frac{n(r)}{r} + \frac{2k^2 k_B T_{Fd}}{k_m r^3} + \frac{k^4 \hbar^2}{4k_m^2 r^6} \right) - \omega_a^2 - \frac{k^2 \left| \bar{E}_d \right|^2}{\left(\frac{e^2}{\varepsilon} \frac{k_z^2}{k_m} \frac{n(r)}{r} + \frac{2k^2 k_B T_{Fd_j}}{k_m r^3} + \frac{k^4 \hbar^2}{4k_m^2 r^6} \right)} \right].$$

Thus the modified total optical nonlinear susceptibility considering multiple size colloids managed by polynomial size distribution function becomes

$$[\chi_t^{(2)}]_M = \chi_e^{(2)} + \int_{r_{\min}}^{r_{\max}} \chi_d^{(2)} dr \,. \tag{32}$$

Therefore for uniform size colloids equation (32) can be conveniently modified by using relations (26) to (28) to get total nonlinear optical susceptibility as

$$[\chi_t^{(2)}]_U = \chi_e^{(2)} + \chi_d^{(2)} \,. \tag{33}$$

It may be inferred from equation (32) that the total crystal susceptibility is influenced and modified by the presence of implanted metal colloids and their distribution; hence colloids and their size distribution are found responsible for the modification in dispersion characteristics of the scattered wave in a parametric process.

3. Results and discussion

To get some numerical appreciation, we consider that an n-InSb crystal is irradiated by a 10.6 μm CO_2 laser (both cw and pulsed beams depending on the intensities required).

Table 1: Material parameters for n-InSb/CO_2 laser system.

Parameter	Symbol	Units	Value
Crystal mass density	ρ	kg m^{-3}	5.8×10^3
Piezoelectric coefficient	β	Cm^{-2}	0.054
Acoustic damping parameter	Γ_a	s^{-1}	2×10^{10}
Acoustic wave velocity	v_a	ms^{-1}	4×10^3
Acoustic wave frequency	ω_a	s^{-1}	2×10^{11}
Stokes wave frequency	ω_s	s^{-1}	1.77×10^{14}
Pump wave frequency	ω_0	s^{-1}	1.78×10^{14}
Electron collision frequency	ν_e	s^{-1}	3.5×10^{11}
Electron's effective mass	M	($\times m_0$)	0.014
Electron;s rest mass	m_0	kg	9.1×10^{-31}
Colloids mass	m_d	kg	1.67×10^{-27}

The physical parameters used are displayed in Table 1. Using these parameters, we have performed qualitative as well as quantitative analysis of colloidal size distribution effect on parametric interaction in IISPs.

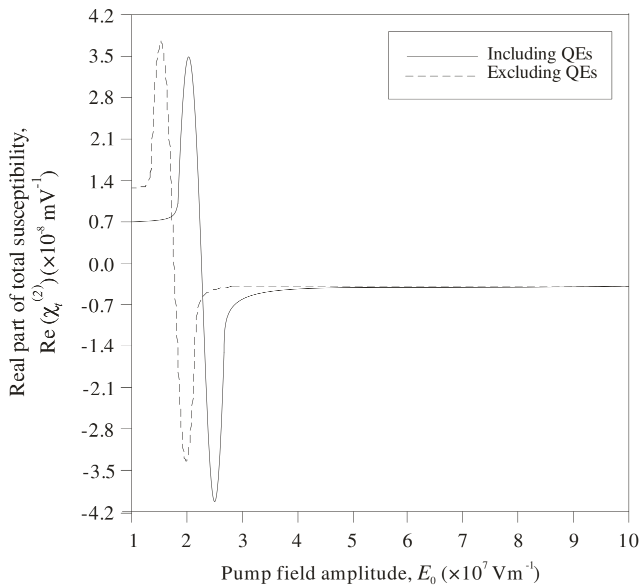

Figure 1: Variation of real part of total susceptibility $\mathrm{Re}[\chi_e^{(2)}]$ with pump field amplitude E_0 for uniform colloids (0.5 nm radius) plasma medium for the cases: (i) excluding QEs, and (ii) including QEs.

Figure 1 shows the variation of real part of total crystal susceptibility $\mathrm{Re}[\chi_t^{(2)}]$ with pump field amplitude E_0 in the presence and absence of quantum correction term. Here to calculate total crystal susceptibility $\mathrm{Re}[\chi_t^{(2)}]$ we have considered uniform colloids having radius 0.5 nm. The quantum correction shows the effective modification in total crystal susceptibility. The shape of both the curves is identical. The magnitude of $\mathrm{Re}[\chi_t^{(2)}]$ first increases with E_0 reaches a maximum value. The value of E_0 at which one gets maximum magnitude of $\mathrm{Re}[\chi_t^{(2)}]$ shifts towards higher side due to the presence of quantum correction but the maximum possible magnitude of $\mathrm{Re}[\chi_t^{(2)}]$ reduces due to the presence of quantum correction. A little departure from this point sharply reduces the value of $\mathrm{Re}[\chi_t^{(2)}]$, reaches to zero, crosses over to negative value and reaches to a minimum. Again, the magnitude of E_0 at which one gets minimum $\mathrm{Re}[\chi_t^{(2)}]$, shifts towards higher point due to the presence of quantum correction term. Beyond this point $\mathrm{Re}[\chi_t^{(2)}]$ starts increasing and saturates towards higher values of E_0. In the saturation region quantum correction becomes negligible or vanishes. The positive and negative values of $\mathrm{Re}[\chi_t^{(2)}]$ may be used to determine wavelength and frequency conversion and to the self-focusing and self defocusing phenomena. It can also be envisaged that a practical demonstration of the above kind of parametric dispersion may lead to the possibility of observation of group velocity dispersion in IISPs and the effect of quantum correction on this dispersion characteristics.

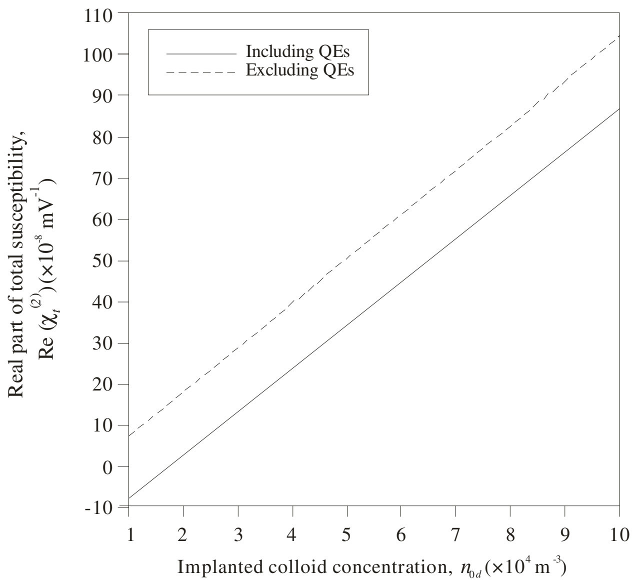

Figure 2: Variation of real part of total susceptibility $\mathrm{Re}[\chi_e^{(2)}]$ with electron concentration n_0 of implanted colloids in uniform colloidal plasma medium for the cases: (i) excluding QEs, and (ii) including QEs.

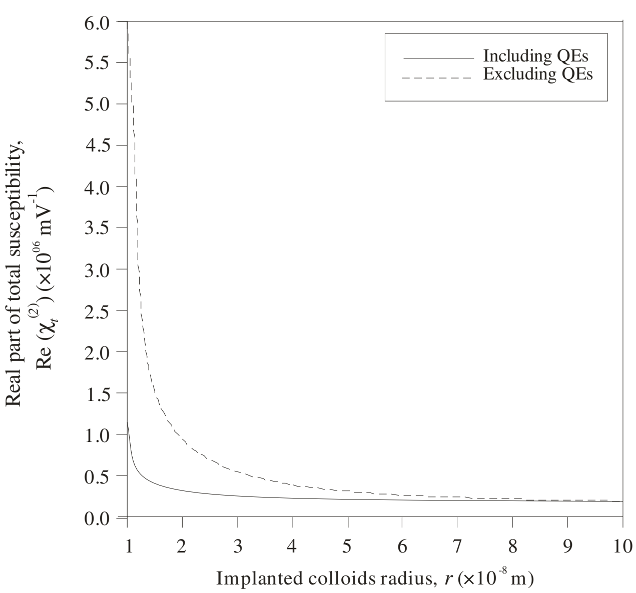

Figure 3: Variation of real part of total susceptibility $\mathrm{Re}[\chi_e^{(2)}]$ with radius r of implanted colloids in uniform colloidal plasma medium for the cases: (i) excluding QEs, and (ii) including QEs.

Figure 2 depicts the variation of real part of total susceptibility $\mathrm{Re}[\chi_t^{(2)}]$ with charged colloids number density with and without QEs for uniform sized colloidal medium. QEs make the sufficient difference with total crystal susceptibility as seen from curve (*b*) of this figure. The total crystal susceptibility in presence of quantum correction for sufficiently lower number density has negative values but without quantum correction crystal susceptibility is always in positive regimes.

Figure 3 envisages the variation of $\mathrm{Re}[\chi_t^{(2)}]$ with radius of colloids ranging from 0.1 to 1 nm. The formulation for real part of total crystal susceptibility $\mathrm{Re}[\chi_t^{(2)}]$ is done by considering the medium consisting of uniform size colloids. Real part of total crystal susceptibility $\mathrm{Re}[\chi_t^{(2)}]$ decreases as we increase the radius of implanted particle till it approaches lattice spacing (≈ 0.6 nm) and beyond this value susceptibility becomes saturated for both the cases, i.e. in presence and absence of QEs. For Colloids with radius more than the lattice spacing (≈ 0.6 nm), the effect of quantum correction vanishes. QEs mainly depend on the mass and size of implanted colloids. The larger mass and size will give rise to smaller QEs. It is also evident from the fact that magnitude of quantum correction term lies in the range 3.3×10^{25} – 1.5×10^{23} till radius of the implanted colloids reaches to lattice spacing. Beyond lattice spacing (r > lattice spacing) quantum correction term decreases effectively up to 3.3×10^{22}. The quantum correction effectively modifies the values of real part of total crystal susceptibility $\mathrm{Re}[\chi_t^{(2)}]$ in IISPs. In our study, it is observed that the magnitude of quantum correction term gradually decreases with increase in the radius of implanted colloids in IISPs. Hence, to study quantum correction on parametric dispersion characteristics the radius of the implanted ions should be kept less than the lattice spacing of the crystal under study.

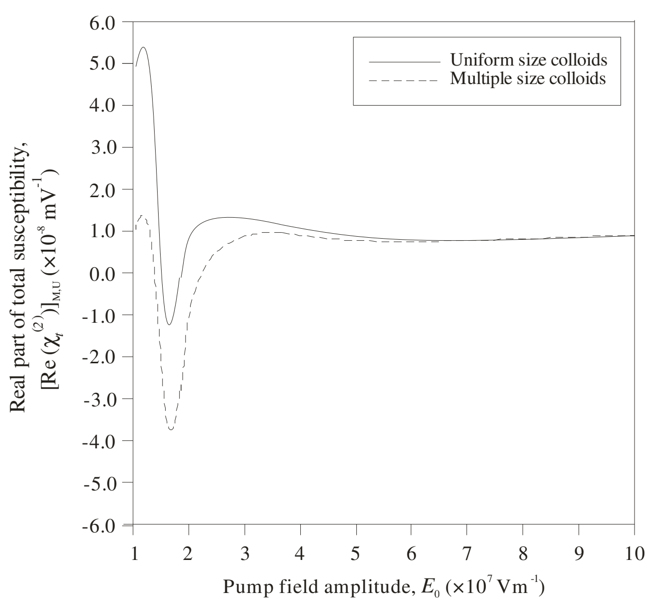

Figure 4: Variation of real part of total susceptibility $\mathrm{Re}[\chi_e^{(2)}]$ with pump electric field E_0 for the cases: (i) uniform size colloids, and (ii) multiple size colloids.

Figure 4 shows the variation of real part of total crystal susceptibility in IISPs with uniform size colloids and multiple size colloids. The differential polynomial expressed distribution function is used for calculating the effect of multiple size colloids in IISPs. Pump field dependent parametric dispersion characteristics are found with distinct anomalous regime. It is observed that in both the cases magnitude of second order susceptibility is positive as well as negative under anomalous regime. For $E_0 < 1.25\times10^7\,\mathrm{Vm^{-1}}$, $\mathrm{Re}[(\chi_t^{(2)})_M]$, $\mathrm{Re}[(\chi_t^{(2)})_U]$ are both positive quantities which initially increases and then achieves a maximum value simultaneously. A slight tuning in E_0 beyond this point both the susceptibilities decrease very sharply, enter the negative quadrant and achieve the minimum value at about $E_0 \approx 1.25\times10^7\,\mathrm{Vm^{-1}}$. With further increase in the value of E_0, both the susceptibilities increase sharply and saturate at larger values of electric field amplitude E_0. At the saturation regime susceptibility due to multiple size colloids $\mathrm{Re}[(\chi_t^{(2)})_M]$ is unable to achieve the positive value again. The magnitude of susceptibility of multiple size colloids medium $\mathrm{Re}[(\chi_t^{(2)})_M]$ is always found less than the magnitude of $\mathrm{Re}[(\chi_t^{(2)})_U]$.

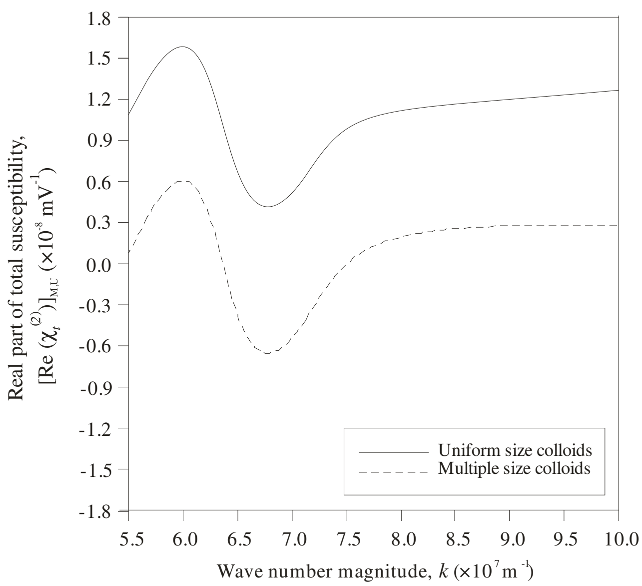

Figure 5: Variation of real part of total susceptibility $\mathrm{Re}[\chi_e^{(2)}]$ with wave number k for the cases: (i) uniform size colloids, and (ii) multiple size colloids.

Figure 5 shows the variation of real part of total crystal susceptibility with wave number k in the cases of uniform size colloids medium and multiple size colloids medium. On increasing the wave vector, the magnitude of $\mathrm{Re}[(\chi_t^{(2)})_M]$, $\mathrm{Re}[(\chi_t^{(2)})_U]$ increase initially and achieves a maximum positive value simultaneously at about $k \approx 5.8\times10^7\,\mathrm{m^{-1}}$. Beyond this point both the quantity decreases very sharply and achieves a minimum value at about $k < 6.7\times10^7\,\mathrm{m^{-1}}$ sequentially. A proper selection of wave vector and grain radius range can enable one to achieve either positive or negative significantly enhanced parametric dispersion in IISPs. The positive and negative values of total crystal susceptibility are used to determine wavelength and frequency conversion and can be directly related to the self-focusing and self-defocusing phenomena. It can also be envisaged that a practical demonstration of the above kind of parametric dispersion may lead to the possibility of observation of group velocity dispersion in IISPs. The polynomial expressed function for colloidal size distribution helps in obtaining the modified dispersion characteristics which may be utilized in the fabrication of microelectronic devices.

4. Conclusions

The nature of the parametric dispersion characteristics of IISPs arising from the real part of total susceptibility, viz. $\mathrm{Re}[\chi_t^{(2)}] = \mathrm{Re}[\chi_e^{(2)}] + \mathrm{Re}[\chi_d^{(2)}]$ of a piezoelectric semiconductor has been reported. The principle objective of the present analysis is to establish the potentiality of the dependency quantum correction term on colloidal size during parametric dispersion process and examine the colloidal size distribution effect on IISPs through QHD model of plasmas. The presence of different sized negative-charged colloids in the IISPs modified the dispersion properties of the shear acoustic waves arising due to the application of pump electric field E_0. Proper selection of the range of colloidal radii may enable one to achieve improved parametric dispersion characteristics in IISPs. The presence of colloids does not contribute towards growth of the signal mode. QHD model is the extended version of hydrodynamic model which includes the quantum correction term which may successfully applied to study the nonlinear optical process in IISPs. The resonance between quantum correction term and electron plasma frequency $(\omega_{pe}^2 + k^2 V_{Fe}^{'2})$ and dust plasma frequency $(\omega_{pd}^2 + k^2 V_{Fd}^{'2})$ is responsible for all the possible changes in parametric characteristics studied. In present study it is found that QEs on colloids is inversely proportional to size, smaller colloids induce larger QEs. QEs on colloids are more effective for certain size of colloids. In our case the limiting size of ion implanted colloids is 0.7 nm which is equal to lattice spacing of the medium. The uniform and multiple size colloid grains and electron dynamics are influenced by Bohm potential in IISPs via QHD model. Inclusion of QEs in QHD model via Bohm potential is seen to play a vital role in the colloid size distribution effect. QEs modify the optical parametric characteristics of IISPs. The quantum correction through Bohm potential effectively modifies the wave propagation characteristics in presence of uniformly sized colloids in the medium.

Acknowledgements

The author is thankful to Dr. Manjeet Singh, Assistant Professor, Department of Physics, Government College, Matanhail (Jhajjar) Haryana, India for useful suggestions, providing support and facilities to carry out this research work.

References

[1] P.K. Gupta, P.K. Sen, The role of electrostriction on parametric dispersion and amplification in doped piezoelectric semiconductors, *Nonlinear Optics* **26** (2001) 361-377.

[2] C. Ciuti, P. Schwendimann, A. Quattropani, Theory of polariton parametric interactions in semiconductor microcavities, *Semicond. Sci. Technol*. **18** (2003) S279.

[3] M. Singh, P. Aghamkar, S.K. Bhakar, Parametric dispersion and amplification in semiconductor-plasmas: effects of carrier heating, *Opt. Laser Tech.* **41** (2009) 64-69.

[4] S. Dubey, S. Ghosh, Parametric oscillations of polaron modes in magnetized semiconductor plasmas, *New J. Phys.* **11** (2009) 093030.

[5] S. Ghosh, S. Dubey, R. Vanshpal, Quantum effect on parametric amplification characteristics in piezoelectric semiconductors, *Phys. Lett. A* **375** (2010) 43-47.
[6] N. Yadav, S. Ghosh, P. Thakur, M. Jamil, M. Salimullah, Parametric interactions in ion-implanted piezoelectric semiconductor plasmas, *Arab. J. Sci. Eng*. **35** (2010) 231-240.
[7] S. Jangra, H.P. Singh, V. Kumar, Acoustical-phonon and polaron mode-induced optical parametric amplification in transversely magnetized III-V semiconductors, *Mod. Lett. Phys. B* **33** (2019) 1950271.
[8] J. Gahlawat, S. Dahiya, M. Singh, High gain coefficient parametric amplification of optical phonon mode in magnetized $A^{III}B^{V}$ semiconductor plasmas, *Arab. J. Sci. Eng*. **46** (2021) 721-729.
[9] M. Singh, A. Sangwan, Sanjay, M. Singh, Parametric oscillation of acoustical phonon mode in magnetized doped III-V semiconductors, *J. Opt*. **50** (2021) 209-222.
[10] D. Singh, B.S. Sharma, M. Singh, Parametric amplification of acoustical phonons in semiconductor magneto-plasmas: quantum effects, *Materials Today: Proc*. **49** (2022) 1383-1389.
[11] E.J. Price, J.E. Walsh, Operation of the grating-coupled oscillator at sub-millimeter/ far-infrared wavelengths, *Appl. Phys. Lett*. **61** (1992) 252-254.
[12] H. Hosono, Y. Abe, N. Matsunami, Coalescence of nanosized copper colloid particles formed in Cu^{+} implanted SiO_2 glass by implantation of fluorine ions: Formation of violet copper colloids, *Appl. Phys. Lett*. **60** (1992) 2613-2615.
[13] N. Matsunami, H. Hosono, Colloid formation effects on depth profile of implanted Ag in SiO_2 glass, *Appl. Phys. Lett*. **63** (1993) 2050-2052.
[14] R.F. Haglund Jr., L. Yang, R.H. Magruder, J.E. Witting, K. Becker, R.A. Zuhr, Picosecond nonlinear optical response of a Cu: silica nanocluster composite, *Opt. Lett*. **18** (1993) 373-375.
[15] M. Salimullah, S. Ghosh, M.R. Amin, Possible lattice formation of new materials within a piezoelectric semiconductor plasma, *Pramana J. Phys*. **54** (2000) 785-789.
[16] M. Salimullah, P.K. Shukla, S.K. Ghosh, H. Nitta, Y. Hayashi, Electron–phonon coupling effect on wake fields in piezoelectric semiconductors, *J. Phys. D: Appl. Phys*. **36** (2003) 958.
[17] M. Salimullah, A.M. Rizwan, S.K. Ghosh, P.K. Shukla, N. Nambu, H. Nitta, Y. Hayashi, Long-ranged order formation of colloids of implanted ions in a dc biased piezoelectric semiconductor, *J. Appl. Phys*. **97** (2005) 124505.
[18] M. Salimullah, Z. Ehsan, K. Zubia, H.A. Shah, G. Murtaza, Possible colloid crystal formation in a magnetized and inhomogeneous semiconductor plasma, *J. Appl. Phys*. **102** (2007) 053301.
[19] S. Ghosh, P. Thakur, Dispersion and absorption of longitudinal electro-kinetic waves in ion-implanted semiconductor plasmas, *Ind. J. Pure & Appl. Phys*. **44** (2005) 235-242.
[20] S. Ghosh, P. Thakur, Effect of drifting carriers on longitudinal electro-kinetic waves in ion-implanted semiconductor plasmas, *European Phys. J. D* **35** (2005) 449-452.
[21] S. Ghosh, P. Khare, Acousto-electric wave instability in ion-implanted semiconductor plasmas, *European Phys. J. D* **35** (2005) 521-526.
[22] I. Zeba, C. Uzma, M. Jamil, M. Salimullah, P.K. Shukla, Colloidal crystal formation in a semiconductor quantum plasma, *Phys. Plasmas* **17** (2010) 032105.
[23] Pravesh, S. Dahiya, D. Singh, M. Singh, Quantum effects on modulational amplification in ion-implanted semiconductor magnetoplasmas, *Pramana J. Phys*. **97** (2023) 58.
[24] Pravesh, S. Dahiya, N. Singh, M. Singh, Dispersion, threshold and gain characteristics of Brillouin scattered Stokes mode in ion-implanted semiconductor quantum plasmas, *Optik* **293** (2023) 171452.
[25] M.G. Ancona, G.J. Iafrate, Quantum correction to the equation of state of an electron gas in a semiconductor, *Phys. Rev. B* **39** (1989) 9536-9540.
[26] P. Meuris, The influence of a dust size distribution on the dust-acoustic mode, *Planet. Space Sci*. **45** (1997) 1171-1174.
[27] F. Verheest, G. Jacobs, T. Cattaert, Dust-acoustic modes in plasmas with dust distributions and charge fluctuations, *New. J. Phys*. **5** (2003) 211-220.
[28] T. Cattaert, F. Verheest, Kinetic theory of dust-acoustic waves in plasmas with dust distributions and charge fluctuations, *IEEE Trans. Plasma Sci*. **32** (2004) 537-541.
[29] J.H. Chen, Effects of dust size distribution on nonlinear waves in a dusty plasma, *Chin. Phys. B* **18** (2009) 2121-2128.
[30] P.K. Kaw, Parametric excitation of ultrasonic waves in piezoelectric semiconductors, *J. Appl. Phys*. **14** (1973) 1497-1498.
[31] G. Manfredi, F. Haas, Self-consistent fluid model for a quantum electron gas, *Phys. Rev. B* **64** (2001) 075316.
[32] F. Haas, L.G. Garcia, J. Goedert, G. Manfredi, Quantum ion acoustic waves, *Phys. Plasmas* **10** (2003) 3858-3866.
[33] D. Bohm, A suggested interpretation of the quantum theory in terms of "hidden" variables I, *Phys. Rev*. **85** (1952) 166-179.
[34] D. Bohm, A suggested interpretation of the quantum theory in terms of "hidden" variables II, *Phys. Rev*. **85** (1952) 180-192.
[35] S. Guha, P.K. Sen, S. Ghosh, Parametric instability of acoustic waves in transversely magnetized piezoelectric semiconductors, *Phys. Stat. Sol. (a)* **32** (1979) 407-414.
[36] P.V. Bliokh, V.V. Yaroshenko, Electrostatic waves in Saturns rings, *Sov. Astron*. **29** (1985) 330-336.
[37] W.S. Duan, Y.R. Shi, The effect of dust size distribution for two ion temperature dusty plasmas, *Solitons and Fractals* **18** (2003) 321-328.
[38] W.S. Duan, H.J. Yang, Y.R. Shi, K.P. Lv, The effects of Gaussian size distribution dust particles in a complex plasma, *Phys. Lett. A* **361** (2007) 368-372.